Influence of Pb impurities on He-bubble formation and growth in Al studied by positron annihilation and transmission electron microscopy

S. G. Usmar*
Brookhaven National Laboratory, Upton, New York 11973

R. N. Wright
Idaho National Engineering Laboratory, EG&G Idaho, Inc., Idaho Falls, Idaho 83415
(Received 25 July 1991; revised manuscript received 9 December 1991)

Positron-lifetime and transmission-electron-microscopy measurements are reported for He (4.5 at. ppm), in pure Al, and Pb-contaminated ($\sim$1 at. ppm) Al:0.5 wt. % Ni alloy. The observed He-bubble growth in pure Al was found to follow at $t^{1/5}$ dependence, i.e., was in good agreement with previously published data. The Pb-contaminated alloy exhibited accelerated He agglomerate and bubble growth. Bubbles observed by transmission electron microscopy in the Pb-contaminated alloy were found to have precipitates attached to them. No precipitates were observed that were not associated with bubbles and no bubbles observed that did not have a precipitate attached. Agglomerate and bubble radii were calculated using the positron-lifetime data. Again the results for pure Al were found to be in good agreement with previously published data. In the Pb-contaminated alloy agglomeration and coalescence occurred at temperatures as low as $\sim$80 °C, while accrual of free volume started at $\sim$180 °C. An increase in bubble growth rate, which occurred between $\sim$350° and $\sim$400 °C, was tentatively associated with the melting of Pb precipitates.

INTRODUCTION

One of the inveterate problems associated with nuclear technology has been the effect of radiation associated with the fission (and possibly in the future, fusion) process on the various structural components of nuclear reactors. Here major technological interest has been focused on the effect of inert gases, produced during nuclear transmutations, which may occur in various parts of a reactor. Such gases are insoluble in metal lattices and usually form gas-vacancy clusters or bubbles at a variety of defect sites such as precipitates, dislocations, and grain boundaries.

Bubble formation and growth contributes to irradiation-induced welling and therefore gives rise to important technological questions. Further, since the relative contributions of the various growth mechanisms are still a matter of some controversy bubble growth is also of intrinsic interest.

Nucleation and growth of He bubbles in high-purity Al has been studied using various techniques. Manzke *et al.*[1] studied He densities within bubbles as a function of annealing temperature, using electron-energy-loss spectroscopy. Bubbles were found to be overpressurized and the authors suggest that growth occurs via thermally activated processes such as thermal vacancy absorption and/or migration and coalescence of bubbles. The transmission-electron-microscopy (TEM) observations of Ono *et al.*[2] led these authors to draw similar conclusions. These authors also determined bubble size distributions at low He concentrations and inferred that growth was by ripening when bubbles densities were not high enough for coalescence to occur.

Helium-bubble growth in Al has also been studied by various workers[3–5] using positron-lifetime spectroscopy (PLS). Notable recent studies have been made by Rajainmaki *et al.*[4] and Jensen *et al.*[5] The former authors employed PLS and TEM and found that two growth regimes existed. In the temperature range 125°–325 °C growth was found to occur by agglomeration and coalescence via bubble migration. Above 325 °C, vacancy absorption as well as agglomeration and coalescence may contribute to bubble growth. Similar conclusion were reached by Jensen *et al.*[5]

These growth mechanisms are also applicable to helium bubbles attached to rigid defects such as solid precipitates and grain boundaries, although in this case bubble migration (and coalescence) is severely restricted due to lower surface energy between the bubble and precipitate compared to that between the bubble and the matrix.[6] When the bubbles are not free to migrate, coarsening is significantly retarded.

In a recent paper[7] TEM and PLS results showing extremely rapid He-bubble growth in an aluminum alloy containing a low concentration [$<$1 at. ppm Ref. (7)] of Pb as an impurity were reported. Here we present further TEM results and a detailed discussion of the PLS data including calculations of bubble radii, volumes, and pressures from these data. The results for the alloy show that (at least for) bubbles large enough for TEM observations had Pb precipitates associated with them. These bubbles were observed to grow much more rapidly than those observed in otherwise identically prepared pure Al. Measured bubble growth in pure Al samples was found to be consistent with previously published data.[8]

EXPERIMENTAL PROCEDURE

Pure Al and Al:0.5 wt. % Ni foils (25×25 mm^2 350 μm) were produced (by cold working and annealing raw materials) and subsequently ion implanted with He^{2+} at the Brookhaven National Laboratory Tandem Van der Graaf facility.[7] After implantation the samples contained $\sim$4.5 at. ppm helium in the central 70 μm of the 350 μm foils and were therefore chemically thinned to approximately 70 μm. Both TEM and PLS samples were prepared from the resulting foils.[7] TEM was carried out in a Philips EM 420 electron microscope while positron-lifetime spectra were accumulated using standard "Fast Fast" coincidence spectrometers[9] with timing resolution of 150 or 170 ps full width at half maximum (FWHM). A full description of the annealing procedures and other experimental details not mentioned here was given in Ref. 7 and references therein.

RESULTS AND DISCUSSION

TEM and Energy dispersive x-ray spectroscopy

Two examples of electron micrographs of helium bubbles in the Al–0.5 wt. % Ni alloy after annealing for 10 h at 500 °C are shown in Fig. 1. It is evident from the micrograph that each of the helium bubbles is attached to a precipitate. These precipitates were found, using EDXS,[7] to be Pb and to take several orientations [also Ref. 7 but note the far left-hand bubble in Fig. 1(a)] with respect to the He bubbles.

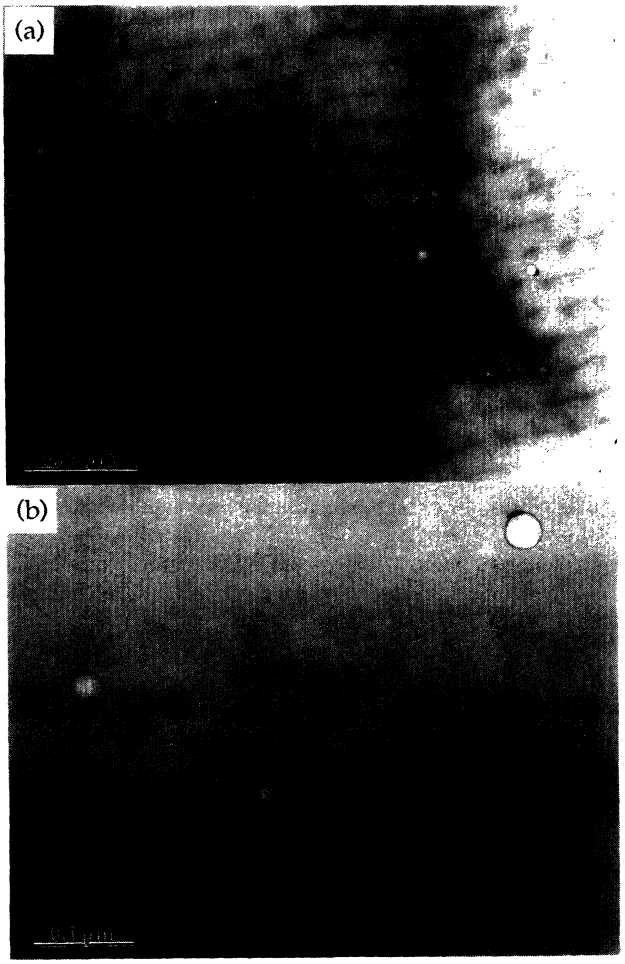

FIG. 1. Bright-field electron micrographs of He bubbles attached to Pb precipitates after annealing for 10 h at 500 °C.

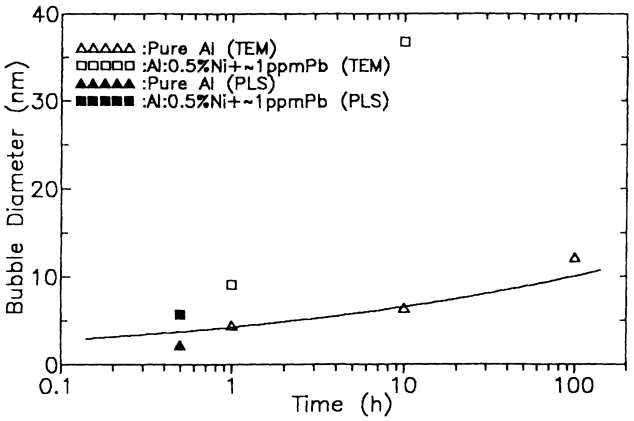

FIG. 2. Mean bubble diameters in pure Al and in the Pb-containing alloy after annealing for up to 100 h at 550 °C. Open and closed symbols are from TEM and PLS data, respectively.

Bubbles sizes were measured for pure Al and alloy samples annealed at 550 °C for 1, 10, and 100 h and calculated for 0.5 h at 550 °C from the PLS results using the method outlined in the next section. The values for both sets of samples are shown in Fig. 2. The solid line in the figure represents the predicted helium-bubble growth rate in pure aluminum assuming that growth is a surface diffusion controlled migration and coalescence process. The predicted values were calculated assuming that the bubble radius is proportional to $t^{1/5}$, using values for the surface diffusion coefficient quoted by Farrell, Chickering, and Mansur.[8] The fit between the values calculated using these assumptions and the measured values is quite good. The bubbles in the Al-Ni alloy containing Pb displayed much faster growth. Rapid bubble coarsening was also observed in the lead-containing alloy after annealing at 500 °C.

Positron-lifetime measurement

A positron-lifetime spectrum[10] generally consists of the sum of at least two decaying exponentials and since not all positrons have sufficient energy to pass through the source window (8 μm Kapton) one of these components is associated with annihilations in the window. Further complications occur because the measured spectra are a convolution of the finite timing resolution of the spectrometer and the real spectrum. Thus numerical analysis of said spectra can only be accomplished with the aid of a nonlinear curve-fitting computer program. Here the program PFPOSFIT,[11] a standard program developed for positron-lifetime analysis, was used. The program returns the reduced chi-squared (χ^2_R) as a measure of the quality of a particular fit. Values of $\chi^2_R \leq 1.15$ are generally accepted as indicating a good fit.

The substructures of as-implanted samples were found,

using TEM, to be complex. Initial numerical analysis of all lifetime spectra was therefore completed using two (excluding source) component fits. In fact, single-component analyses were tested at various stages and were found to return $\chi_R^2 \geq 2.0$. The positron annihilation parameters τ_2 (lifetime) and I_2 (relative intensity) for pure Al and Al:0.5 wt. % Ni are plotted in Figs. 3(a) and 3(b), respectively. The two sets of data show marked differences. Data for pure Al are in good agreement with previously published work.[3-5] Here two distinct annealing stages, separated by a plateau (in τ_2) between $\sim$340 and $\sim$400 °C, are apparent. The alloy exhibits a low-temperature plateau and subsequent monotonic behavior in the temperature range ($\sim$80–600 °C) studied. Evidently the data for τ_2 and I_2 are in very good agreement, throughout the temperature range studied, for both samples of Al:Ni alloy studied. The data for the two samples of pure Al show a similar agreement for τ_2 but I_2 diverges above 340 °C. This divergence probably arose because of the differences in the loss of defects (He) at surfaces which in turn resulted from different sample thickness brought about by inconsistencies in chemical thinning.

Values of χ_R^2 returned by PFPOSFIT were found, for pure Al, to be quite poor ($0.976 \leq \chi_R^2 \leq 1.465$) below 340 °C and good ($0.985 \leq \chi_R^2 \leq 1.15$) above 340 °C, suggesting two-component fitting to be inappropriate below 340 °C. Two-component fits for the alloy data resulted, with a few scattered exceptions, in $0.985 \leq \chi_R^2 \leq 1.15$ throughout the temperature range studied. Application of the two-state trapping model[12,13] allows a further and somewhat more concise test of the validity of two-component fitting. Here the bulk positron lifetime can be related to measured positron-lifetime parameters (τ_1, τ_2, I_1, and I_2):

$$\tau_b = (I_1\lambda_1 + I_2\lambda_2)^{-1} , \quad (1)$$

where $\lambda_i = \tau_i^{-1}$.

Thus the bulk lifetime for Al, which is constant and has been measured as 157±5 ps, can be calculated. In Fig. 4 τ_b calculated using Eq. (1) has been plotted versus temperature for pure Al and Pb containing Al:Ni alloy. For pure Al the two-state trapping model is only valid above $\sim$370 °C, here calculated and measured values of τ_b are in good agreement. Thus in pure Al samples multiple defect types are active positron traps at annealing temperatures below $\sim$370 °C, while only He-vacancy agglomerates survive above this temperature. The He-vacancy agglomerates coarsen into bubbles as the annealing temperature is increased.

The calculated and measured values of τ_b for the alloy samples are in good agreement throughout the temperature range (20–600 °C) studied. This implies that, for the alloy samples, there only existed a single active positron trap which evolved with annealing temperature. Above 350 °C the trap was most definitely a He bubble which coarsened as the annealing temperature was increased. Below 350 °C the traps must be regarded as He-vacancy agglomerates and will simply be referred to as agglomerates henceforth. Agglomerate and He-bubble radii can be calculated from the positron-lifetime data using the theoretical model of Nieminen and Laakkonen[14] and empirical expression of Jensen *et al.*[5] for positron trapping rates into agglomerates and/or bubbles, respectively, in conjunction with the molecular-dynamics theory of Jensen and Nieminen.[15,16] Calculated bubble radii for pure Al and the Pb-contaminated alloy are plotted versus temperature in Fig. 5. The calculations assumed that no He was lost throughout the temperature range studied for all but the second pure Al sample. For this sample it was assumed that the $\sim$30% reduction of I_2 below that for sample one, at 370 °C, was a result of He loss and that no further He loss occurred in sample 2. Further all the He was assumed to be contained in agglomerates and/or bubbles. The calculated bubble radii were found to be in good agreement with those observed by TEM (cf Fig. 2), for both the pure Al and the Pb-contaminated alloy. Further, the present results for pure Al are consistent

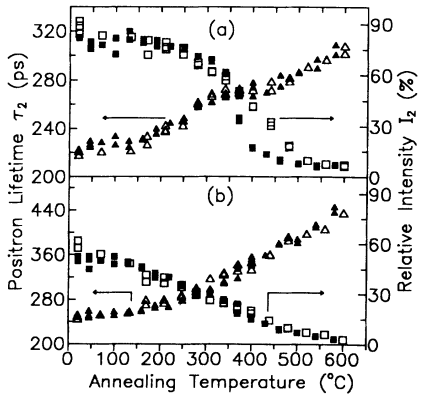

FIG. 3. The lifetime and fractional intensity of the long-lived component of the positron annihilation spectra as a function of annealing temperature for (a) pure Al and (b) the Al:Ni alloy containing $\sim$1 ppm Pb as an impurity. Open and closed symbols are data from samples 1 and 2, respectively.

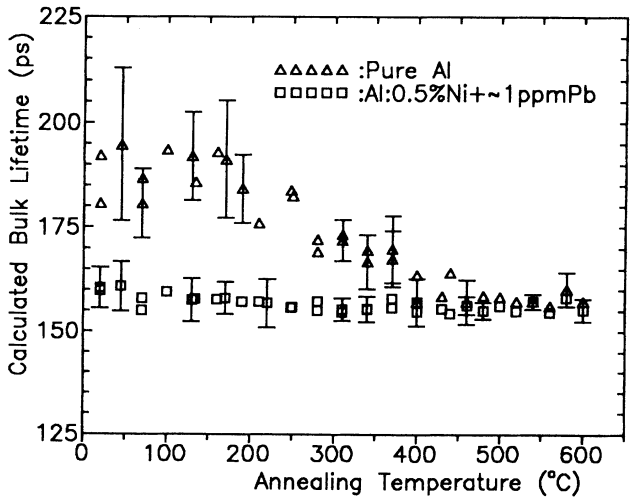

FIG. 4. Calculated bulk positron lifetime as a function of annealing temperature for pure Al and Pb-contaminated alloy.

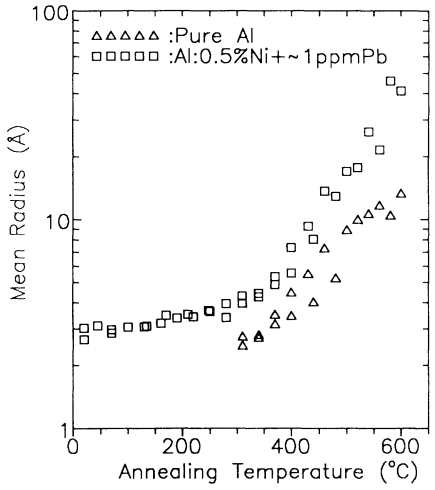

FIG. 5. He agglomerate and bubble radii (calculated using the PLS data) vs annealing temperature for pure Al and the Pb-contaminated alloy.

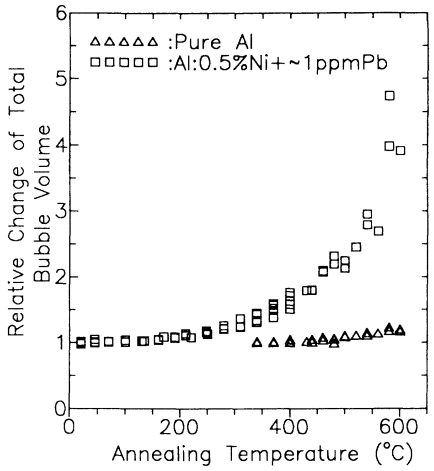

FIG. 6. Relative change in total bubble volume (normalized at 340 °C and 20 °C for pure Al and Pb-contaminated Al:Ni alloy, respectively) as a function of annealing temperature for pure Al and Pb-contaminated alloy.

with previously published data.[3-5]

Before proceeding it should be noted that the theory of Jensen and Nieminen[16] has been shown[5] to give good quantitative values for average bubble radii ≥ 0.5 nm of He bubbles in Al. Calculations of agglomerate radii are, however, less precise than those for bubbles. Recent advances in the theory for empty cavities and agglomerates[16-18] suggest that reliable calculations for He-vacancy agglomerates will become possible in the near future. With respect to the present results it should be noted that theory[16] used to calculate He densities in bubbles will when used for agglomerates overestimate this number and thus underestimate the bubble radii. Regardless of the problems associated with these calculations it is evident from the variations of τ_2 and I_2 [Fig. 3(b)] with temperature that agglomerates in the Pb-contaminated alloy start to evolve at temperatures as low as ~80 °C. In pure Al agglomerates do not evolve below ~350 °C.

Further information pertaining to bubble growth can be obtained by calculation the relative change in total bubble volume, which is just

$$V_R = \left[\frac{N_{\mathrm{He}T}}{n_{\mathrm{He}b}}\right] V_{\mathrm{in}}^{-1} , \tag{2}$$

where V_{in} is the initial total agglomerate or bubble volume; $N_{\mathrm{He}T}$ is the total He concentration and $n_{\mathrm{He}b}$, which can be written as[5,16]

$$n_{\mathrm{He}b} = (500 - \tau_2)/23.5 , \tag{3}$$

is the average He density in the bubbles and is in units of (10^{28} m^{-3}) and τ_2 is the β^+ lifetime in ps. The relative volume change is plotted versus temperature in Fig. 6. V_{in} was taken so that $V_R = 1$ at 340 °C and 20 °C for pure and Pb-contaminated Al, respectively. (Note that for pure Al there are multiple active positron traps below ~340 °C.)

Below ~450 °C and ~360 °C for pure Al and Pb-contaminated alloy, respectively,these data should be regarded with some scepticism. The values of $n_{\mathrm{He}b}$ [given by Eq. (3)] used when calculating bubble radii and relative volume change in this temperature range are most probably incorrect. However, if the observed temperature dependences of agglomerate radii and fractional volume change are unaltered by advances in the theory, then the following is clear. Below ~500 °C and ~180 °C evolution of agglomerates in pure Al and Pb-contaminated alloy, respectively, occurs by agglomeration and coalescence. That the agglomerates evolve is clear from the observed variation [Fig. 3(a) and 3(b)] in the positron annihilation parameters τ_2 and I_2. Here the decrease of I_2 with increasing temperature corresponds to a reduction in the density of positron traps, i.e., agglomerates.

Above ~180 °C for Pb-contaminated alloy and ~500 °C for pure Al the relative agglomerate and/or bubble volume increases. For pure Al the volume increase occurs in the regime where $r_b \geq 0.5$ nm, i.e., where calculated values of r_b ($n_{\mathrm{He}b}$), are reliable. The volume change is, however, quite small amounting to ~15%. In the Pb-contaminated alloy both bubble radii and relative volume most certainly increase above ~360 °C. Thus it must be concluded that above 180 °C subject to the previously noted conditions pertaining to theoretical calculations of bubble radii and relative volume the growth mechanism must include injection of open volume into bubbles. Again it should be recognized that even in the absence of a theory the raw positron-lifetime data [Fig. 3(b)] would, at least qualitatively, support this conclusion. Here the observed increase of τ_2 can only be accounted for if the average He density in agglomerates and/or bubbles decreases and since He desorption from agglomerates and bubbles is impossible bubble or agglomerate volumes must be increasing. Also since the relative intensity I_2 [Fig. 3(b)] of the positron lifetime τ_2 decreases throughout the temperature range ~180–600 °C it must be concluded that agglomeration

and coalescence of agglomerates and/or bubbles also occurs throughout this temperature range. Thus the present results indicate that above 360 °C and 500 °C for Pb-contaminated alloy and pure Al, respectively, bubble growth occurs via agglomeration and coalescence and accrual of additional volume. Further these processes are greatly enhanced by the presence of Pb precipitates on bubbles, i.e., in the Pb-contaminated alloy. The volume change in pure Al amounts to $\sim 15\%$ while that for the alloy is $\sim 350\%$.

The mechanism by which agglomerates and/or bubbles accrue free volume is unclear. For pure Al a comparison of equilibrium and actual gas pressures for temperatures ≥ 460 °C reveals (see Fig. 7) that below ~ 500 °C equilibrium pressures are equal to calculated gas pressures, while above this temperature these pressures have a constant ratio within experimental error of 0.65. Here gas pressures were calculated using the values of $n_{\mathrm{He}b}$ obtained using Eq. (3) in conjunction with the empirical equation of state (EOS) of Mills, Lievenberg, and Bronson,[19] which according to Donnelly[20] provides an "acceptable means of describing the behavior of helium over a large range of temperature and pressure." Equilibrium pressures were calculated with the surface energy of Al taken as[20] 1.03 $\mathrm{J\,m^{-2}}$. Evidently this result cannot account for the observed bubble expansion in Al unless the EOS overestimates the gas pressure in bubbles by a factor of ~ 1.6. If this were the case then the ratio of equilibrium to gas pressure would fall from ~ 1.6 at 480 °C to a value of 1.0 at 500 °C and above. The data would then be consistent with bubble expansion via thermal vacancy trapping when, after coalescence, the gas pressure was larger than the equilibrium pressure.

With respect to the validity of calculated gas pressures the following can be said. The method used to calculate gas pressures here and elsewhere (Ref. 20 and references therein) has been to apply a macroscopic EOS obtained from classical thermodynamic data to what is a microscopic system. In other words the calculations do not account for finite-size effects[21] and assume a uniform gas density inside the helium bubbles. Such effects are pertinent to bubbles of radius ≤ 10 nm, which, it is generally agreed,[22] is the limit above which significant finite-size effects disappear. Indeed such effects might account, at least in part, for the enormous (up to 50 GPa) calculated gas pressures which have lead some authors (e.g., Fenske[23]) to assume that not all He was contained in observable bubbles. Thus gas pressures reported for bubbles with radii ≤ 10 nm using the EOS method are most probably incorrect and need to be reevaluated. As an example of nonuniform gas densities the authors note that the molecular-dynamics calculations completed by Jensen and Nieminen[16] clearly illustrate the nonuniformity of He in bubbles, e.g., with $n_{\mathrm{He}b} = 5.8 \times 10^{23}$ $\mathrm{cm^{-3}}$ the surface density of helium was found to be 9.2×10^{23} $\mathrm{cm^{-3}}$.

Since the fractional surface area of Pb on the bubbles in the Pb-contaminated alloy cannot be estimated for the present work and may well be temperature dependent (i.e., change as the precipitates passes through its liquids) equilibrium bubble pressures cannot be calculated. Helium gas pressures, calculated using the EOS of Mills, Lievenberg, and Bronson,[19] for bubbles in the Pb-contaminated alloy for temperatures above 360 °C are plotted versus temperature in Fig. 8. Evidently bubble pressures decrease as the annealing temperature increases. The surface energy of Pb (~ 0.43 $\mathrm{J\,m^{-2}}$) is approximately half that of Al (~ 1.03 $\mathrm{J\,m^{-2}}$). Further evaluation of equilibrium bubble pressures for the Pb-contaminated alloy, assuming that surface energies were unaltered by the presence of the Pb, results in equilibrium pressures which are higher than the calculated gas pressures, e.g., at 580 °C $P_{\mathrm{equ}} \sim 0.55$ GPa while $P_{\mathrm{gas}} \sim 0.2$ GPa. Thus it is tentatively suggested that the Pb precipitates present on He bubbles in the Pb-contaminated alloy lower the surface energy of said bubbles to such an extent that they become over pressurized at much lower temperatures than in pure Al. Further it

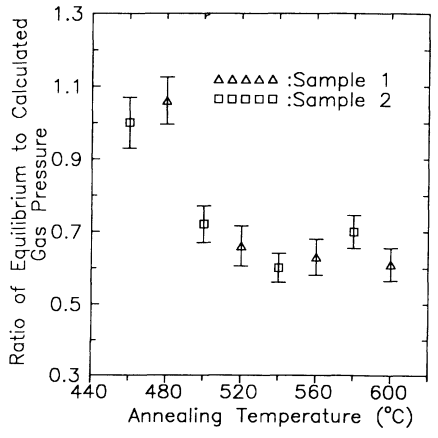

FIG. 7. Ratio of equilibrium pressure ($2\gamma/r$) to He gas pressure calculated using the EOS of Mills, Lievenberg, and Bronson (Ref. 19) vs annealing temperature for pure Al.

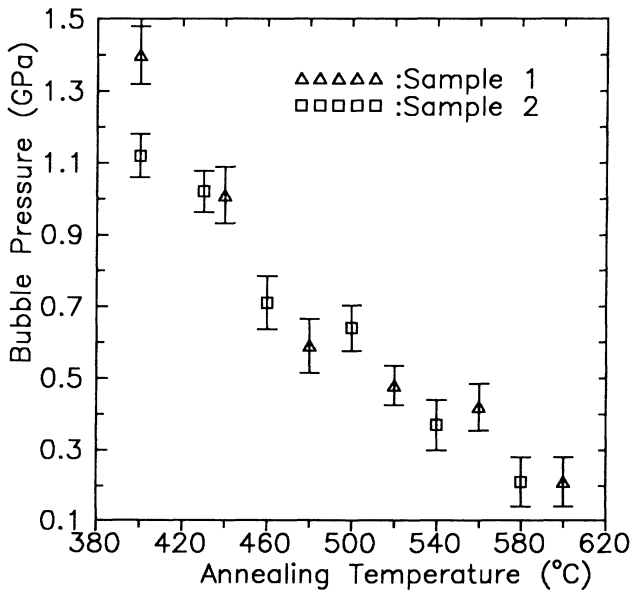

FIG. 8. He gas pressure calculated using the EOS of Mills, Lievenberg, and Bronson (Ref. 19) vs annealing temperature for bubbles in Pb-contaminated Al:0.5 wt. % Ni alloy.

appears that the presence of Pb precipitates on bubbles enhances bubble mobility.

The mechanism for enhanced mobility is at present unclear. However, the work of Delamare and Rhead[24] on the effect of adsorbed layers of Pb on the surface diffusion of Cu and Au suggests a possible mechanism. Here it was found that the presence of adsorbed Pb layers enhances surface diffusion of both Cu and Au. Thus, since bubble growth in pure Al occurs via surface diffusion controlled agglomeration and coalescence it is tentatively suggested that the presence of Pb enhances diffusion of Al at agglomerate and bubble surfaces thereby increasing agglomerate and bubble mobility and consequently agglomerate and bubble growth. The increase in growth rate of bubble radii which occurs between ~350 and ~400 °C (Fig. 5), although not particularly well defined, can be seen as qualitative support for the above mechanism. Since bulk Pb melts at 327.65 °C Gråbaek *et al.*[25] have demonstrated the microscopic Pb precipitates in Al may have melting temperatures up to 70 °C above that for the bulk it is tentatively suggested that the increased growth rate of bubbles, which occurs in the temperature range ~350–~400 °C, results from the Pb precipitates melting. On melting the Pb most probably redistributes itself around the entire bubble thus modifying the surface properties of the bubble. The nebulous nature of the increase in growth rate may result from the observed distribution (cf. Fig. 1) of bubble and precipitate sizes.

Now one important question pertaining to the relationship between the He and Pb remains unanswered. Namely do the He agglomerates and/or bubbles trap mobile Pb atoms during annealing or do the Pb impurity atoms act as He traps during implantation. Since TEM observations revealed all observed Pb precipitates to be associated with He bubbles one might conclude that Pb traps He during implantation. Here the bubble growth data obtained from the PLS studies are also useful. The fact that agglomerate growth in the Pb-contaminated alloy starts at temperatures as low as 20 °C suggests that Pb was present on agglomerates and bubbles throughout the annealing sequence, i.e., that Pb atoms acted as He traps during implantation.

CONCLUSION

From the above discussion it must be concluded that the Pb precipitates associated with He bubbles in the alloy containing Pb as an impurity enhance He bubble growth. Raw PLS data, calculated average radii, and relative agglomerate and/or bubble volume suggest that growth occurs via agglomeration and coalescence starting at temperatures as low as ~80 °C. Above ~180 °C agglomerate and bubble growth also occurs, as is evident from the change in the relative agglomerate and/or bubble volume (cf. Fig. 6), by accrual of additional free volume.

The underlying mechanisms responsible for enhanced agglomerate and bubble growth are, at the present time, unclear. However, two possible processes have been tentatively identified. With respect to accrual of free volume, it appears that the presence of Pb precipitates on agglomerates and bubbles reduces the surface energies of said entities. Thus agglomerates and bubbles probably become overpressurized at much lower temperatures (i.e., smaller radii) than in pure Al. Consequently growth via accural of free volume starts at much lower temperatures than in pure Al.

It has been suggested, with the peripheral support of previously published data,[24] that the presence of Pb precipitates increases the surface diffusivity of Al around agglomerates and bubbles. Thus if, as is the case for pure Al, bubble growth occurs via surface diffusion controlled agglomeration and coalescence, the increased surface diffusivity of Al in the presence of Pb precipitates would explain the enhanced agglomerate and bubble growth observed in the Pb-contaminated alloy. The increase in bubble growth rate which occurs between ~350° and ~400 °C in the Pb-contaminated alloy can be explained if the Pb precipitates melt in this temperature range. It should be noted that the above conclusions are somewhat speculative and that further studies of He bubble growth in the presence of Pb and other low melting point precipitates, e.g., In are necessary to test them fully.

Finally it must be said that the calculated gas pressures reported here and elsewhere for bubbles of radius ≤ 10 nm must be reevaluated with finite-size effects taken into account.

ACKNOWLEDGEMENTS

The author gratefully acknowledges the assistance of C. Carlson and co-workers at the BNL Tanden van de Graaff Facility for their assistance with He ion implantation. This work was supported at INEL by the U.S. Department of Energy, Office of Basic Energy Sciences under DOE Contract No. DE-AC07-761DO1570. Analytical electron microscopy was carried out in the Center for Microanalysis, University of Illinois, which is supported by the U.S. Department of Energy under Contract No. DE-AC02-76ER 01198. One of the authors (S.G.U.) would also like to thank the SERC (U.K.) for their support through SERC Contract No. GRF 49491.

---

*Current address: University of Bristol, H. H. Wills Physics, Laboratory, Royal Fort, Tyndall Avenue, Bristol, BS8 1TL, U.K.

[1]R. Manzke, G. Crecelius, W. Jager, H. Trinkaus, and R. Zeller, Radiat. Eff. **78**, 327 (1983).

[2]K. Ono, M. Inoue, T. Kino, S. Furuno, and K. Izui, J. Nucl. Mater. **133&134**, 477 (1985).

[3]C. L. Snead, A. N. Goland, and F. W. Wiffen, J. Nucl. Mater. **64**, 195 (1977).

[4]H. Rajainmaki, S. Linderoth, H. E. Hansen, R. M. Nieminen, and M. D. Bentzon, Phys. Rev. B **38**, 1087 (1988).

[5]K. O. Jensen, M. Eldrup, B. N. Singh, and M. Victoria, J. Phys. F **18**, 1069 (1988).

[6]R. S. Nelson, J. Nucl. Mater. **19**, 149 (1966).

[7]R. N. Wright, C. D. Van Siclen, S. G. Usmar, and M. E. Mochel, J. Nucl. Mater. **182**, 281 (1991).

[8]K. Farrell, R. W. Chickering, and L. K. Mansur, Philos Mag. **53**, 1 (1986).
[9]W. H. Hardy II and K. G. Lynn, IEEE Trans. Nucl. Sci. **23NS**, 229 (1976).
[10]For background and reviews the reader is referred to R. N. West, *Positron Studies of Condensed Matter* (Taylor Francis, London, 1974); R. N. West, in *Positrons in Solids,* edited by P. Hautojarvi, Topics in Current Physics, Vol. 12 (Springer-Verlag, New York, 1979); p. 89; *Positron Solid State Physics,* edited by W. Brandt and A. Dupasquier (North-Holland, New York, 1983).
[11]W. Puff, Comput. Phys. Commun. **30**, 359 (1983).
[12]B. Bergersen and M. J. Stott, Solid State Commun. **7**, 1203 (1969).
[13]D. C. Connors and R. N. West, Phys. Lett. **30A**, 245 (1969).
[14]R. M. Nieminen and J. Laakkonen, J. Appl. Phys. **20**, 181 (1979).
[15]K. O. Jensen and R. M. Nieminen, Phys. Rev. B **35**, 2087 (1987).
[16]K. O. Jensen and R. M. Nieminen, Phys. Rev. B **36**, 8219 (1987).
[17]M. S. Puska and R. M. Nieminen, J. Phys. F **13**, 333 (1983).
[18]K. O. Jensen and A. B. Walker, J. Phys. F **18**, L277 (1988).
[19]R. L. Mills, D. H. Lievenberg, and J. C. Bronson, Phys. Rev. B **21**, 5137 (1980).
[20]S. E. Donnelly, Radiat. Eff. **90**, 1 (1985).
[21]J. S. Rowlinson and B. Widom, *Molecular Theory of Capillarity* (Oxford University Press, New York, 1982).
[22]R. Evans (private communication).
[23]G. Fenske, Ph.D. thesis, University of Illinois, 1979 (unpublished).
[24]F. Delamare and G. E. Rhead, Surf. Sci. **28**, 267 (1971).
[25]L. Gråbaek, J. Bohr, E. Johnson, A. Johansen, L. Sarholt-Kristensen, and H. H. Andersen, Phys. Rev. Lett. **64**, 934 (1990).

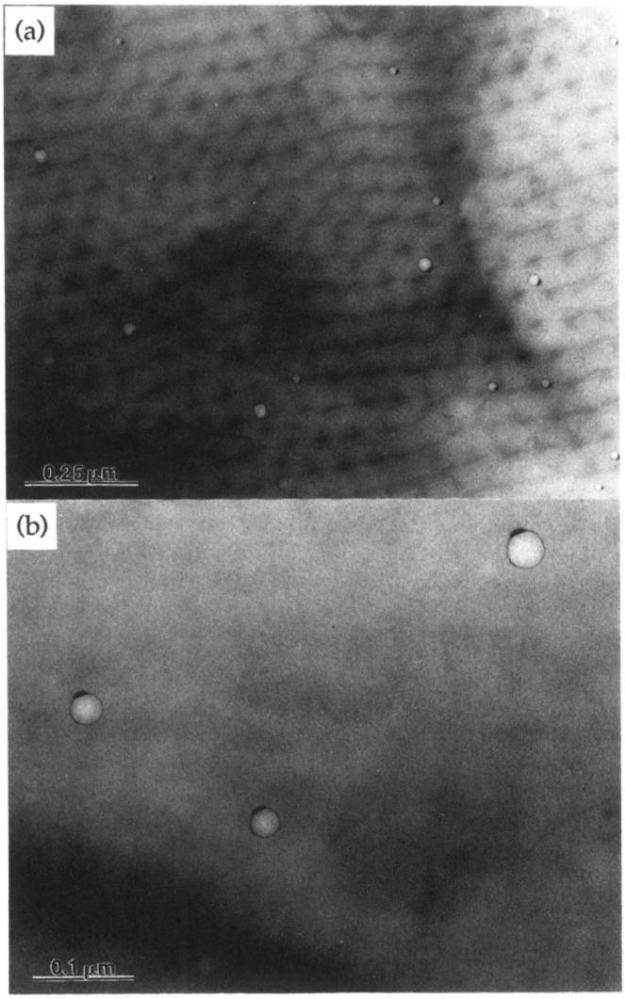

FIG. 1. Bright-field electron micrographs of He bubbles attached to Pb precipitates after annealing for 10 h at 500 °C.